LASER
& PHOTONICS
REVIEWS

Laser Photonics Rev. **8,** No. 4, L47–L51 (2014) / **DOI** 10.1002/lpor.201300200

LETTER
ARTICLE

Abstract The optical switch is a key component in photonic integrations that plays an important role in routing the optical signal within a photonic circuit. In this work, compact switches were proposed and demonstrated based on the interference of surface plasmons polaritons (SPP) on free metal surfaces and in waveguides. Thanks to the constructive and destructive interferences implemented in strip waveguides, 2 × 2 ports switch devices with a small footprint were achieved with a maximum modulation depth of about 80%. Moreover, an interesting composite interference was observed and analyzed in the waveguide device, which is considered to arise from a transmission/reflection interference and field superposition interference. The samples of Bragg gratings and slits with different parameters were investigated in detail, which provided convincing evidence supporting the composite interference model. This revealed that the mechanism would possibly inspire new designs and instructions in nanophotonic integrations.

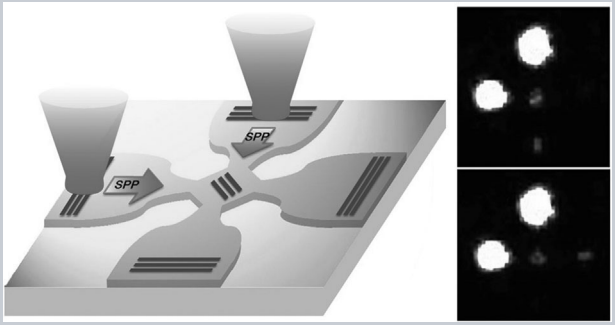

Plasmonic switch based on composite interference in metallic strip waveguides

Yulin Wang, Tao Li*, Lei Wang, Hao He, Lin Li, Qianjin Wang, and Shining Zhu

Optical computing has been pursued for decades as a potential strategy in developing new information technology beyond the fundamental limitations of semiconductor-based electronic devices. Thanks to the compressed wavelength, the surface plasmon polariton (SPP), an electromagnetic bounded wave propagating along a metal/dielectric interface, is regarded as a promising carrier to downsize the conventional optical elements and even to realize all-optics circuits [1–3]. Among the various optical interconnects, the compact switch is an important device in photonic integrations, which enables the signal to be turned on and off by another controller, and is fundamentally used to construct the optical logic gates [4–6].

Here, we will first demonstrate a plasmonic switch based on the interference of SPPs by a Bragg grating as the beam splitter (BS) in a planar silver surface, as schematically depicted in Fig. 1b. Next, we will extend this design to the plasmonic strip waveguides [7]. Besides the switching functionality in a more compact manner, a new interference mechanism is exploited, which is found to give rise to a shifted interference compared with the planar one. Our results not only provide us with an effective plasmonic switch with low fabrication requirement, but also reveal two kinds of interference mechanisms within the plasmonic waveguides that would possibly offer guidance in developing new plasmonic devices.

As has been illustrated in Fig. 1b, the plasmonic switch contains four gratings on a metal surface as couplers between the incident laser and SPPs, whose grating constant is designed according to the SPP wavelength λ_{SPP}. A 45° titled Bragg grating is designed located along the diagonal line of the device, which is made of three grooves with a period of $\lambda_{SPP}/\sqrt{2}$ for a 90° reflection of the SPP wave. With careful design of the parameter of Bragg grating, it can allow for a half-to-half reflection and transmission of SPPs by neglecting the scattering loss. In principle, this plasmonic switch is designed on the basis of a Mach–Zehnder interferometer [8, 9]. The central BS (Bragg grating) can cause a phase shift δ between transmitted and reflected SPPs. For a half-to-half symmetric splitter, this δ is equal to $\pi/2$ according to the Degiorgio relation [10]. Defining the phase of incident SPP in two inputs (Ports I and II) as α and β, we can get the phase differences between the two branches of SPPs in two output ports (III and IV) as $\phi_1 = \alpha-\beta+\pi/2$ and $\phi_2 = \alpha-\beta-\pi/2$, respectively. Then, the output powers of these two ports can be deduced as,

$$\begin{aligned} I_3 &= I_{1t} + I_{2r} + 2\sqrt{I_{1t}I_{2r}}\cos\phi_1 \\ I_4 &= I_{2t} + I_{1r} + 2\sqrt{I_{2t}I_{1r}}\cos\phi_2. \end{aligned} \quad (1)$$

In our optical setting, the initial phase difference $(\alpha-\beta)$ between two incident SPPs can be tuned by a Babinet compensation prism in one branch of the optical path, see Fig. 1a. When $\alpha-\beta = n(\pi/2)$ (n is an odd number), ϕ_1 and ϕ_2 will be equal to either 0 (2π) and $\pm\pi$, or vice versa. In an ideal splitting condition, i.e. $I_{1t} = I_{1r} = I_{2t} = I_{2r}$, the SPP energy in the output ports (III and IV) will result in complete interference as maximum in one port and minimum in the other. Therefore, we can modulate the SPP signals in the output ports by tuning input SPP phase in port I or

National Laboratory of Solid State Microstructures, School of Physics, College of Engineering and Applied Sciences, Nanjing University, Nanjing 210093, China

*Corresponding author: e-mail: taoli@nju.edu.cn

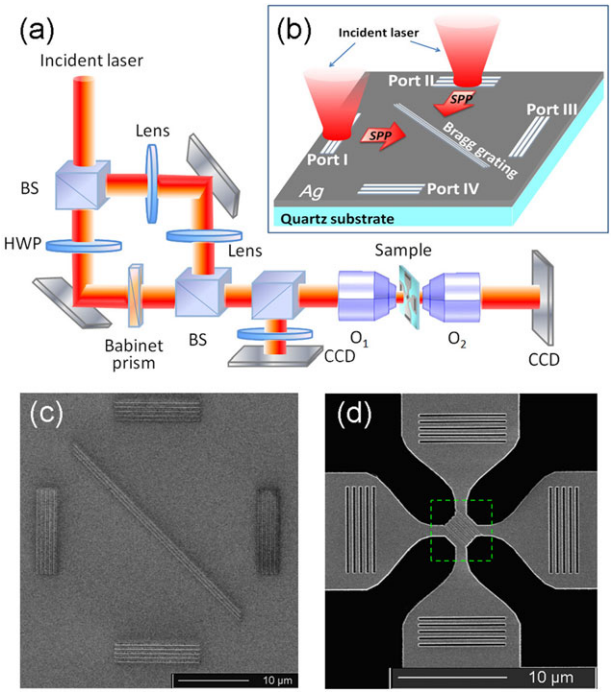

Figure 1 (a) Optical set-up for measurement of the interference of the plasmonic switch device. (b) The schematic structure of the plasmonic switch on a flat metal surface, where the 2×2 ports and Bragg grating are marked out. (c) Scanning electron microscope (SEM) image of the top view of the planar switch sample corresponding to the design of (b). (d) A further developed compact switch based on the strip waveguides, where the Bragg grating still exists in the center cross region (marked with a green dashed box).

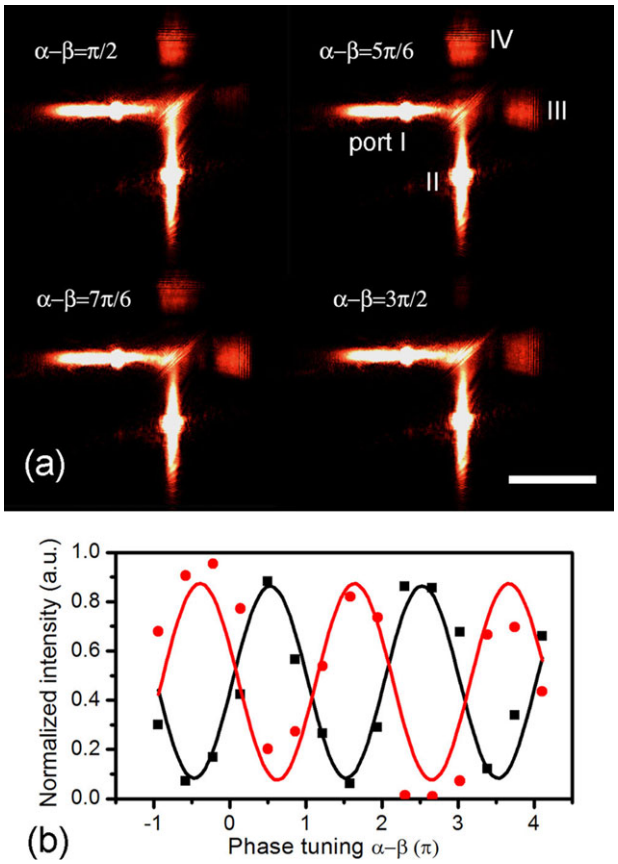

Figure 2 (a) Detected interference at different phase tunings in the planar switch device. Scale bar is 20 μm. (b) Interference results recorded at two output ports (black and red ones correspond to Ports III and IV, respectively), where the symbols are recorded data and the curves are the fitted ones.

II. In this regard, a phase tuned plasmonic switch will be realized via the full optical interference.

In experiments, the Bragg grating BS and all coupling gratings were fabricated on a 100-nm thick silver layer on a quartz substrate via the focus ion beam (Strata FIB 201, FEI company) etching. According to the wavelength of $\lambda_{SPP} = 610$ nm (a He-Ne laser of $\lambda_0 = 632.8$ nm), periods of the coupling gratings and Bragg grating are set as 610 nm and 431 nm, respectively. The occupation ratio of coupling gratings is set to 50% to achieve a good efficiency [11]. All depths of the coupling gratings are 100 nm, while the Bragg grating is set at 20 nm depth to reduce the scattering loss. The top view of whole device is shown in Fig. 1c, where the distance between two horizontal ports is 25 μm, and the whole device has a footprint of about 30×30 μm^2. In the next step, we further minimized the whole device by using strip waveguides as shown in Fig. 1d. These waveguides are expected to confine SPPs into a more compact region. Figure 1a depicts the optical set-up for the analyses. A He-Ne laser beam is split into two branches by a BS. A Barbinet prism is inserted in one branch to tune the phase after a polarization conversion by a half-wave plate (HWP). A pair of lenses are introduced in the other branch to regulate the focusing spot on the sample. After a combination by another BS, two collimated laser beams are focused to Ports I and II of the sample by an objective (O_1, 50×, NA = 0.55). Another oil-immersed objective (O_2, 100×, NA = 1.25) is used on the transmitted side to detect the leakage radiation for the planar sample, which has been commonly used in SPP analyses [12–14]. For these waveguide samples, the switching effect is analyzed in reflections by O_1 to avoid the influence of strong illuminations from the blank area beside the waveguides on the transmission side.

First, we investigated the interference of SPPs in the planar structure (see Fig. 1c). In measurements, the input of Port II was kept fixed, while the phase of another branch to Port I was tuned by adjusting the Babinet prism, so that the phase delay of SPPs between Ports I and II changes. Figure 2a shows four typical states of the interference, from which we find the Ports III and IV are selectively lightened according to different phase tuning. To quantitatively evaluate the interference performance, more data were recorded and plotted in Fig. 2b, which show good interference curves with a modulation depth >80% (defined as $(I_{max} - I_{min})/(I_{max} + I_{min})$). Moreover, it is clear that the intensities of Ports III and IV oscillate almost antisynchronously, which are in coincidence with the Degiorgio principle [10].

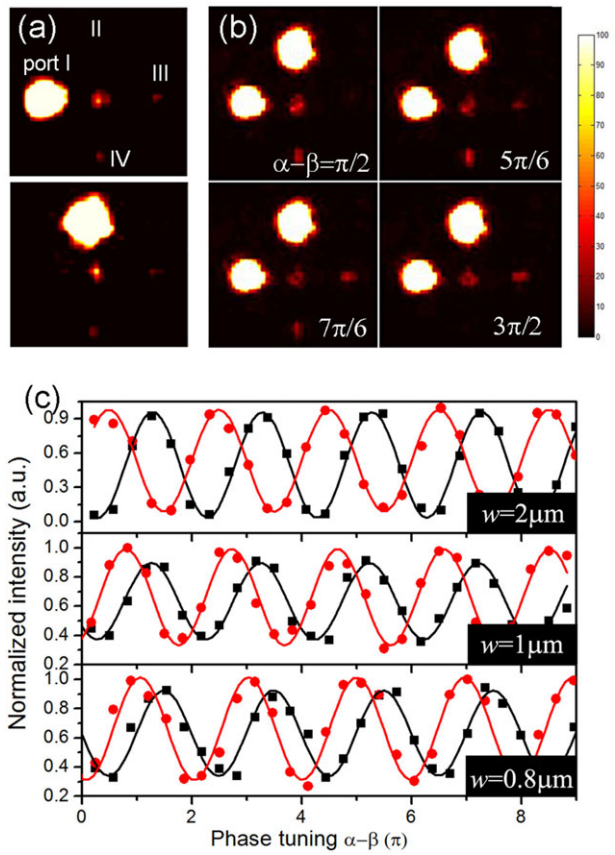

Figure 3 (a) Beam splitting results from Ports I and II, showing an almost half-to-half BS ratio. (b) Detected interference result of waveguide switch $w = 1$ μm on the reflection side (by objective O_1) with respect to different phase tuning. Scale bar is 10 μm. (c) Detailed experimental results of interference of Port III (black) and IV (red) for the waveguide samples ($w = 2$, 1, and 0.8 μm), where obvious shifts are observed as the waveguide narrows down.

Although this plasmonic switch on a flat metal surface has shown very good performance, in a practical sense, people are always seeking more compact devices for photonic integration. Therefore, a waveguide-based switch is more desirable. Figure 1d shows a 2×2 ports switch composed of strip waveguides, in which the BS is shortened within a small cross region (the green box in an area $\sim 6 \times 6$ μm^2). In experiments, samples with three waveguides widths ($w =$ 2, 1, and 0.8 μm) were mainly studied. All interference results were obtained from the reflection side by the objective of O_1, as has been explained. With a checked half-to-half BS property of the Bragg grating in Fig. 3a, Fig. 3b shows the switch results of the sample with $w = 1$ μm, where the Ports III and IV are turned on and off alternately by the phase of Port I. By carefully analyzing the interference data of all samples, it is found that the sample of $w = 2$ μm is almost as same as the planar one, showing good modulation depth ($\sim$80%) and nearly antisynchronous oscillation, as depicted in Fig. 3c. However, the interference curves for samples of $w = 1$ and 0.8 μm manifest an obvious shift as the waveguide narrows down. This interference shift is really interesting, which was seldom discovered or discussed previously. It has been demonstrated that the transmission–reflection (T–R) interference is antisynchronous, as shown in Fig. 2b, which would be reasonably preserved in a symmetric system even within waveguides [10]. However, it seems to shift the interference to a synchronous one as the waveguides narrow down. There must be another factor participating in the contribution. To find out another underlying mechanism, a possible way is to decrease the BS reflection so as to suppress the T–R interference, and reducing the slits of Bragg grating is a convenient means in experiments.

Therefore, we fabricated another series of samples with a single slit to replace the BS of the Bragg grating, as the image shown in Fig. 4a (for the $w = 1$ μm sample). By adjusting the slit depth (with a fixed slit width of 100 nm), we found 50 nm appropriate to achieve good interference. In consequence, a large T/R ratio ($\sim$3.5) was found for the one input case (see Fig. 4b for the $w = 1$ μm sample) that indicates a well-suppressed reflection. The interference results of three samples with $w = 2$, 1, and 0.8 μm are depicted in Fig. 4c. As expected, in absence of reflection, strong interferences of two outputs still occur (modulation depth $\sim$0.7), and they tend to oscillate synchronously as the waveguide width decreases (see the result of $w = 0.8$ μm). Additional experiments showed that further decreasing the slit depth would dramatically weaken the interference depth (for an extreme case, the interference disappears without the slit). It is also the reason that we did not set the slit depth to be the same as that in the previous Bragg grating (20 nm). According to these results, it is ready to accept that this synchronous interference is inevitably related to the contribution of slit in narrow strip waveguides.

A probable explanation for this is that in the narrow strip the SPP (strip-SPP) launched from a single input port will be remarkably transmitted through the tiny slit straight to the output port with little reflection, and the slit-SPP can be barely coupled due to the mismatch of the k directions. However, when two orthogonal strip-SPPs are launched from two input ports (e.g., I and II) simultaneously, the slit-SPP will be efficiently coupled propagating along the slit due to the composite k vectors. In this case, the in-plane field component ($E_{//}$, i.e. E_x+E_y) plays the major role in superposition interference, as schematically shown in Fig. 5a. In fact, according to the vectorial nature of the SPP field, $E_{//}$ and E_z are correlated that can be unified in the definition of slit-SPP. When $E_{//}$ on two slit sides oscillate in phase, strong antiphased normal components E_z are generated beside the slit and also propagate along the slit. This energy will be markedly transferred to strip waveguides towards two outputs (Ports III and IV), resulting in constructive interference. On the contrary, antiphased $E_{//}$ will be considerably inhibited inside the slit, which leads to a destructive interference with the decreased E_z on the strip. Consequently, the slit-SPP mode should have a mode width that depends on the interference states (see Fig. 5a). Probably, due to the presence of the slit-SPP mode width ($w_{\text{slit-spp}}$), this field superposition interference would be

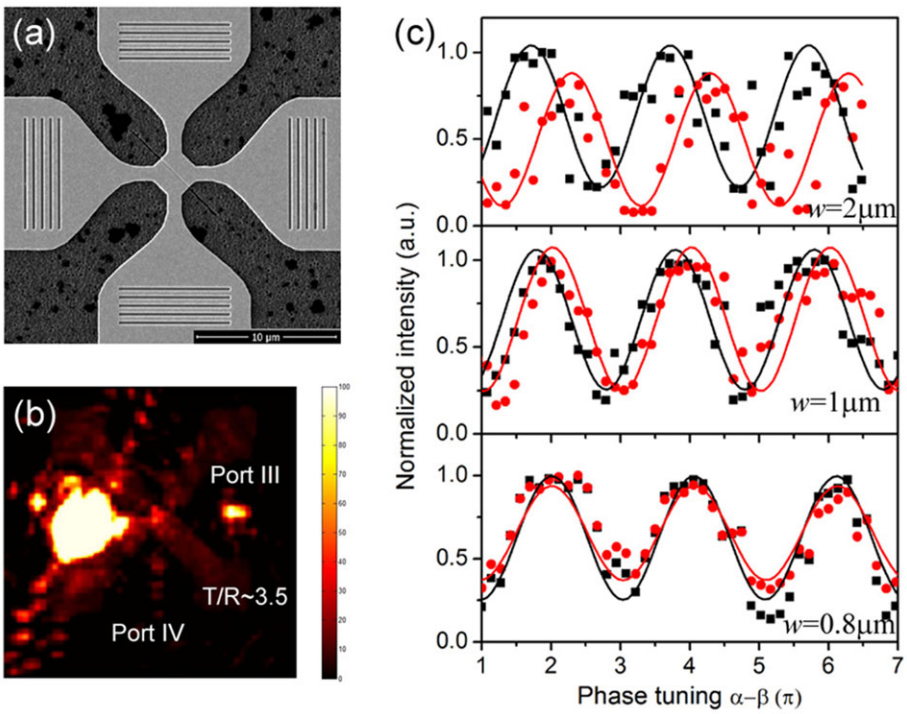

Figure 4 (a) SEM image of the slit-waveguide sample of $w = 1$ μm. (b) Experimental beam splitting result of this sample, showing a large T/R ratio~3.5. (c) Interference results of Port III (black) and IV (red) for the slit samples ($w = 2$, 1, and 0.8 μm), where a synchronous tendency is clearly shown as the waveguide narrows down.

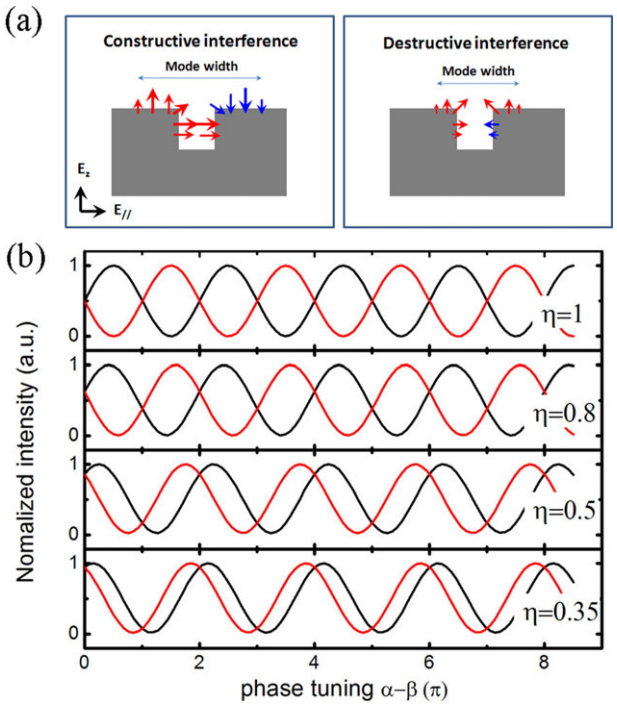

Figure 5 (a) Schematics of field distribution of slit-SPP mode in the case of constructive and destructive interferences, where the mode width of the slit-SPP are marked out. (b) Calculated interference curves based on the composite mechanism, where the proportion of T–R interference is set as $\eta = 1$, 0.8, 0.5, 0.35, respectively.

influenced by the width of the strip waveguide (w). If the waveguide is narrow enough (e.g., $w < w_{\text{slit-spp}}$), this slit-SPP will be uniformly transferred from the cross to waveguides for the inphase case and gives rise to the synchronous interference. When the strips get wider there would be more reflected field beside the slit-SPP mode, which may contribute to the interference besides the superposition. Then, the T–R interference grows up and leads to a tendency to be antisynchronous one. It is well proved by our experiments (see Fig. 4c), and also verified by our numerical simulations (see Supplementary Materials).

Now, with good recognition of two different kinds of interferences, we can describe them in a combined model. For the Bragg grating samples, although the T–R interference has a major contribution, the field superposition inside the slits of the grating may also have a certain amount especially in the narrow waveguides. According to the Degiorgio relation [10], the direct transmitted and reflected field can be defined by

$$E_{1t} = t_1 E_1 \cos(\omega t + \alpha),\ E_{1r} = r_1 E_1 \cos\left(\omega t + \alpha + \frac{\pi}{2}\right), \tag{2a}$$

$$E_{2t} = t_2 E_2 \cos(\omega t + \beta),\ E_{2r} = r_2 E_2 \cos\left(\omega t + \beta + \frac{\pi}{2}\right), \tag{2b}$$

where t and r are the transmission and reflection coefficients, respectively. In the waveguide cases, the E field can be decomposed into two parts: the directed transmitted and reflected field, and that from the superposed slit-SPP. In the

presence of these two kinds of interferences, we can define the T–R part as a proportion of η. Then, there would be a remaining proportion $(1–\eta)$ involved in the field superposition (neglecting the scattering loss for an ideal consideration). Supposing the slit-SPP (mainly the E_z part) is transferred equally to waveguides towards two outputs (Ports III and IV), the corresponding E field can be defined as

$$E_{3s} = E_{4s} \approx \frac{1}{\sqrt{2}}(1-\eta)(E_1 + E_2). \tag{3}$$

Therefore, the intensities in Ports III and IV via the composite interference can be written as

$$I_3 \propto |E_3|^2,\ E_3 \propto E_{1t} + E_{2r} + E_{3s}, \tag{4a}$$

$$I_4 \propto |E_4|^2,\ E_4 \propto E_{2t} + E_{1r} + E_{4s}. \tag{4b}$$

In a symmetric system, setting $t_1 = r_1 = t_2 = r_2 = \frac{1}{\sqrt{2}}\eta$ and $E_1 = E_2$, we can evaluate the interference behavior with different proportions of η. Figure 5 clearly shows a tendency of the interference from antisynchronous to synchronous, as η decreases from 1 to 0.35, which almost reproduces the experimental results. So far, plasmonic switches based on waveguides have been demonstrated with good performance and compact integration. Moreover, this 2×2 switch device can be regarded as two combined logic gates or operators with versatile functionalities (see Supplementary Materials).

In summary, we have developed a series of 2×2 ports plasmonic switches based on the interference of SPPs in both planar metal surface and strip waveguides. A large modulation depth has been achieved in switching the SPP signal by phase tuning. More importantly, besides the switching functionality, a new composite interference mechanism is revealed, for the first time to our knowledge, which gives rise to a shifted interference depending on the waveguide width. It would probably inspire new modulating methods on the guided SPPs and hold the possibility for designing new types of photonic devices at the micro/nanoscale.

Acknowledgements. This work was supported by the National Key Projects for Basic Researches of China (No. 2012CB921501), the National Natural Science Foundation of China (Nos. 11174136, 11322439, 11321063, 91321312), and Dengfeng Project B of Nanjing University.

Supporting Information: for this article is available free of charge under http://dx.doi.org/10.1002/lpor.201300200

Received: 30 November 2013, **Revised:** 10 May 2014, **Accepted:** 12 May 2014

Published online: 11 June 2014

Key words: Surface plasmon polariton, plasmonic switch, interference, strip waveguide.

References

[1] E. Ozbay, Science **211**, 189 (2006).
[2] S. A. Maier, Plasmonics: Fundamentals and Applications (Springer, New York, 2007), p. 107.
[3] Z. Y. Li, Front. Phys. **7**, 601 (2012).
[4] H. Wei, Z. P. Li, X. R. Tian, Z. X. Wang, F. Cong, N. Liu, S. P. Zhang, P. Nordlander, N. J. Halas, and H. X. Xu, Nano Lett. **11**, 471 (2010).
[5] H. Wei, Z. X. Wang, X. R. Tian, M. Käll, and H. X. Xu, Nature Commun. **2**, 387 (2011).
[6] Y. L. Fu, X. Y. Hu, C. C. Lu, S. Yue, H. Yang, and Q. H. Gong, Nano Lett. **12**, 5784 (2012).
[7] S. I. Bozhevolnyi, Plasmonic Nanoguides and Circuits (Pan Stanford, Denmark, 2009), p. 19.
[8] H. Ditlbacher, J. R. Krenn, G. Schider, A. Leitner, and F. R. Aussenegg, Appl. Phys. Lett. **81**, 1762 (2002).
[9] A. Drezet, A. Hohenau, A. L. Stepanov, H. Ditlbacher, B. Steinberger, F. R. Aussenegg, A. Leitner, and J. R. Krenn, Plasmonics **1**, 141 (2006).
[10] A. Zeilinger, Am. J. Phys. **49**, 882 (1981).
[11] I. P. Radko, S. I. Bozhevolnyi, G. Brucoli, L. MartnMoreno, F. J. Garca-Vidal, and A. Boltasseva, Phys. Rev. B **78**, 115115 (2008).
[12] A. Drezet, A. Hohenau, A. L. Stepanov, H. Ditlbacher, B. Steinberger, N. Galler, F. R. Aussenegg, A. Leitner, and J. R. Krenn, Appl. Phys. Lett. **89**, 091117 (2006).
[13] A. Hohenau, J. R. Krenn, A. Drezet, O. Mollet, S. Huant, C. Genet, B. Stein, and T. W. Ebbesen, Opt. Exp. **19**, 25749 (2011).
[14] L. Li, T. Li, S. M. Wang, C. Zhang, and S. N. Zhu, Phys. Rev. Lett. **107**, 126804 (2011).